ANTICANCER RESEARCH *24*: 2601-2616 (2004)

Acute Changes in U937 Nuclear Ca^{2+} Preceding Type 1 "Apoptotic" Programmed Cell Death due to MK 886

K.M. ANDERSON[1,2], M. RUBENSTEIN[1,2], W.A. ALREFAI[3], P. DUDEJA[3], P. TSUI[1] and J.E. HARRIS[4]

[1]Hektoen Institute, Departments of [2]Biochemistry and of [4]Medicine, Rush University Medical Center; [3]Department of Physiology, University of Illinois and West Side V.A. Chicago, IL, 60612, U.S.A.

Abstract. *Background: MK 886, a 5-lipoxygenase inhibitor, induces a type 1 "apoptotic" form of programmed cell death in Bcl-2-positive U937 monoblastoid cells. In Ca^{2+}-depleted, non-permeabilized U937 cells studied with MK 886 in a Ca^{2+}-free medium, an acute increase in Ca^{2+} occured within 10 to 20 seconds, detected with fura-2 measured with a spectrofluorimeter. Methods and Results: The increased fluorescence was nuclear in location, as judged by confocal microscopy. The antioxidant, N-acetyl-L-cysteine, three agents that inhibit mitochondrial function at identified sites, antimycin A, atractyloside and cyclosporin A , the L/N-channel inhibitor, loperamide and BAPTA, an intracellular Ca^{+} chelator pre-loaded into cells each reduced the extent or prevented the acute MK 886-induced rise in Ca^{2+}, as determined by radiometric detection. Rhodamine-2, a more selective mitochondrial Ca^{2+} probe, provided no evidence for nuclear Ca^{2+} originating from that extra-nuclear site or from the endoplasmic reticulum. With 2',7'- dichloro-dihydrofluorescein-labelled cells to detect reactive oxygen species, MK 886 increased the initial fluorescent signal from a number of intracellular, largely extra-nuclear sites, including mitochondria. Two chemicals that inhibit the function of Bcl-2, HA14-1 and 2-methyl-antimycin A3, reduced the Ca^{2+} response to MK 886, if pre-incubated with the Bcl-2-positive U937 cells at 37°C for several hours. MK 886 was previously shown to induce reactive oxygen species and a fall in mitochondrial membrane potential in both Bcl-2-positive U937 and in Bcl-2-negative PC-3 prostate and panc-1 pancreatic cancer cells. The latter solid tumor cells undergo an atypical "type 2" PCD without an acute rise in nuclear Ca^{2+}. Conclusion: These results are consistent with an MK 886-induced increase of reactive oxygen species from intra-cellular sites including mitochondria which release Ca^{2+} located primarily at or near nuclei. These events may involve Bcl-2, participating in some form of Ca^{2+} channel and nuclear Ca^{2+} binding proteins undergoing conformational changes due to reactive oxygen species. Reasons for the different PCD responses in Bcl-2 positive lympho-hematopoietic compared to Bcl-2-negative solid cancer cell lines, respectively with and without the induced nuclear Ca^{2+} signal, remain to be defined.*

Abbreviations: BAPTA-AM, 1,2-bis(2-amino-5-fluorophenoxy (ethane-N,N,N',N'-tetraacetic acid tetrakis(acetoxymethyl) ester; CRE, cyclic AMP response element binding protein; CREB, cyclic AMP response element binding protein; IP_3, 1,4,5,trisinositol phosphate and related congeners; IP_3R, IP_3 receptors; MAPK, MAP kinase; MM, mitochondrial membrane; MMP, mitochondrial membrane potential; MMPT, mitochondrial membrane permeability transition; MPT, mitochondrial permeability transition; NF-AT, nuclear factor for activating transcription; PCD, $PCD_{1\ or\ 2}$, programmed cell death; RNS, reactive nitrogen species; ROS, reactive oxygen species; SRE, serum response element.

Correspondence to: Dr. Ken Anderson, c/o Dr. Marvin Rubenstein, Hektoen Institute, 2100 W Harrison, Chicago, IL 60612, U.S.A. Tel: 847-864-3559, e-mail: marander427@MSN.com

Key Words: MK 886, U937 nuclear Ca^{2+}, apoptosis.

Micro-molar concentrations of the 5-lipoxygenase inhibitor, MK 886, induce a "type 1" form (1) of programmed cell death in human Bcl-2-positive U937 monoblastoid cells (2). This is associated with a rapid increase in cellular Ca^{2+}, occurring within 10-20 seconds that, under the restrictive conditions employed, appears to be largely nuclear in location (3). In Bcl-2-negative human Panc-1 pancreatic cancer cells cultured with MK 886, no acute Ca^{2+} response preceded the development of a "type 2" form of cell death (4). These pancreas cells exhibited a distinctive ultra-structure and were caspase-negative, differing in these ways from the type 1 programmed cell death induced in them by actinomycin D (5). Whether Bcl-2 modulates U937 cellular and especially nuclear Ca^{2+}, as has been reported in other types of cells such as the Dunning G prostate carcinoma (6), has not been established.

The role of ionized calcium as a second messenger-modulator of transcription, the sources of imported or *in situ* nuclear Ca^{2+}, details of its uptake or release, proximate mechanisms through which transcription is modulated and subsequent effects on DNA synthesis, proliferation or the induction of PCD are discussed in recent papers and reviews

(7-26). From this body of information, much of it based on studies of "excitable" muscle or central nervous system cells, an overview of nuclear Ca^{2+} dynamics emerges, some details of which need not apply to other types of cells (18).

Nuclear Ca^{2+} is considered to originate from cytosol, juxta-nuclear and nuclear sources, including the adjacent nuclear envelope and its lumen (7-9,15-17,23,25,26). Major generic features of the latter two sources include the continuity between the intra-nuclear and peri-nuclear space encompassed by the inner and outer leaves of the nuclear envelope and the endoplasmic reticulum (7), the location of calcium-ATPase, a SERCA 2b- related pump on the outer nuclear leaf regulated by a cAMP PKA, calmodulin, IP3 and IP3 receptors and GTP-dependent and ranodyne/cADPr forms of Ca^{2+} uptake by nuclei with 1,4,5-trisphosphate (InsP3)- sensitive ranodyne receptor L-type voltage-activated channels on the inner leaf. Nuclear membrane "pores" for larger (10 kD) molecules and other channels for smaller molecules and ions both exhibit differential regulation (9,11). The recent reports of an intra-nucleoplasmic reticular network connected with the peri-nuclear and ER systems for calcium storage and signaling in SKHep 1 epithelial cells containing $InsP_3$ receptors is especially relevant (15,16,25). In this study, upon stimulation with IP3, intra-nuclear Ca^{2+} increased in localized areas before changes in cytosol Ca^{2+}, followed by translocation of nuclear PKC to the nuclear envelope and movement of cytosol PKC to the nuclei.

Nuclei from diverse types of cells contain tyrosine, MAP and calmodulin-dependent protein kinases, the phosphatase, calcineurin and receptors for 1,4,5-trisphosphate. Differential transcription, dependent upon increased nuclear rather than cytosol Ca^{2+}, has been demonstrated (12,14). The cyclic AMP-response element (CRE) and the CRE-binding protein, CREB in ATt20 cells function as a response element sensitive to nuclear Ca^{2+}-dependent transcription, distinct from transcription due to the serum-response element (SRE) sensitive to cytosolic Ca^{2+}. In a DNA micro-array study of calcium uptake-deficient and control T cells, a central role for the type 2B phosphatase, calcineurin, in Ca^{2+}-positive and Ca^{2+}-negative modulation of gene expression was demonstrated (22). In this T-cell receptor-mediated apoptosis, Ca^{2+}-activated calmodulin associated with cytoplasmic calcineurin which de-phosphorylated a number of early transcription factors, including NFAT and various intermediate-early genes such as c-fos. Nuclear Ca^{2+} signaling in cortical neurones *via* voltage-activated L-type calcium channels included a calmodulin complex that activated the MAP kinase pathway (20). A cyclic AMP response-element was activated by a Ras/mitogen -responsive MAPK pathway. The general conclusion from these and other studies is that Ca^{2+} present at different intracellular sites and released by diverse signals generates differential transcription.

Table I. *Acute effects of some agents of interest on MK 886-induced Ca^{2+} measured with a spectrometer. Any changes in fluorescence were recorded after exposure to the agents of interest for 50 seconds, followed by MK 886 to a final concentration of 40 μM.*

Agents that inhibited or prevented the rise in Ca^{2+}	
antimycin A (inhibits e$^-$ transfer at complex III, cyto C to B1)	10 μM
atractyloside (inhibits ADP/ATP, adenine nucleotide transport, release of cytochrome C, opens permeability transpores)	25 μM
loperamide (Ca^{2+} L/N channel inhibitor)	10 μM
cyclosporin A (inhibits phosphatase 2B and nitric ox syn, inhibit mito. perm. trans pore opening)	10 μM
N-acetyl-cysteine (antioxidant)	50 μM
Agents without acute (within 3 min) effects on Ca^{2+}.	**Concentration**
H_2O_2 (oxidizing agent)	0.1%
NTBN (free radical spin trap)	100 μM
butylated hydroxy-toluene	100 μM
mercapto ethanol	100 μM
dithiothreitol	100 μM
sodium arsenate (uncouples oxidative phos)	100 μM
sodium cyanide (inhibit terminal e- transport)	2 μM
nifedipine (Ca^{2+} channel blocker, 1,4r dihydropyridine type)	5 μM
ionomycin (Ca^{2+} ionophore)	5 μM
thapsigargin (inhibits E.R. ATPase, IP3 Ca^{2+} release)	10 nM
BAPTA (intracellular Ca^{2+} chelator)	100 μM
2-methyl-antimycin A3 (Bcl-2 inhibitor)	10 nM
wortmannin (IP3 kinase inhibitor)	50 μM
SC 41661A (5-lipoxygenase inhibitor)	40 μM
theophyllin (phosphodiesterase ihhibitor	100 μM
caffeine (cAMP phosphopdiesterase inhibitor	100 μM
indomethacin (cyclooxygenase inhibitor)	100 μM
Agents excluded from cells.	**Concentration**
superoxide dismutase	3000 U/ml
catalase	200 U/ml
peroxidase	5000 U/ml
Agents reported to inhibit Bcl-2 function that reduced the Ca^{2+}–response following incubation with cells at 37˚C.	
HA 14-1	24 μM
2-methyl-antimycin A_3	5 μM

As the basis for the studies reported below, our hypothesis was that MK 886 induced the formation, probably primarily in mitochondria, their major intracellular source, of reactive oxygen (or possibly nitrogen) species. These diffuse to nuclei and evoke a major acute release of Ca^{2+} at or near that site. Some nuclear Ca^{2+} might also originate from mitochondria, a major calcium storage site or from the endoplasmic reticulum. In an effort to reduce the potentially confounding movement of Ca^{2+} from multiple intra- and from extra-cellular sources, we used the restrictive conditions of studying Ca^{2+}-depleted, non-permeabilized U937 cells in a Ca^{2+}-free medium. We accepted the fact that some intracellular Ca^{2+}-

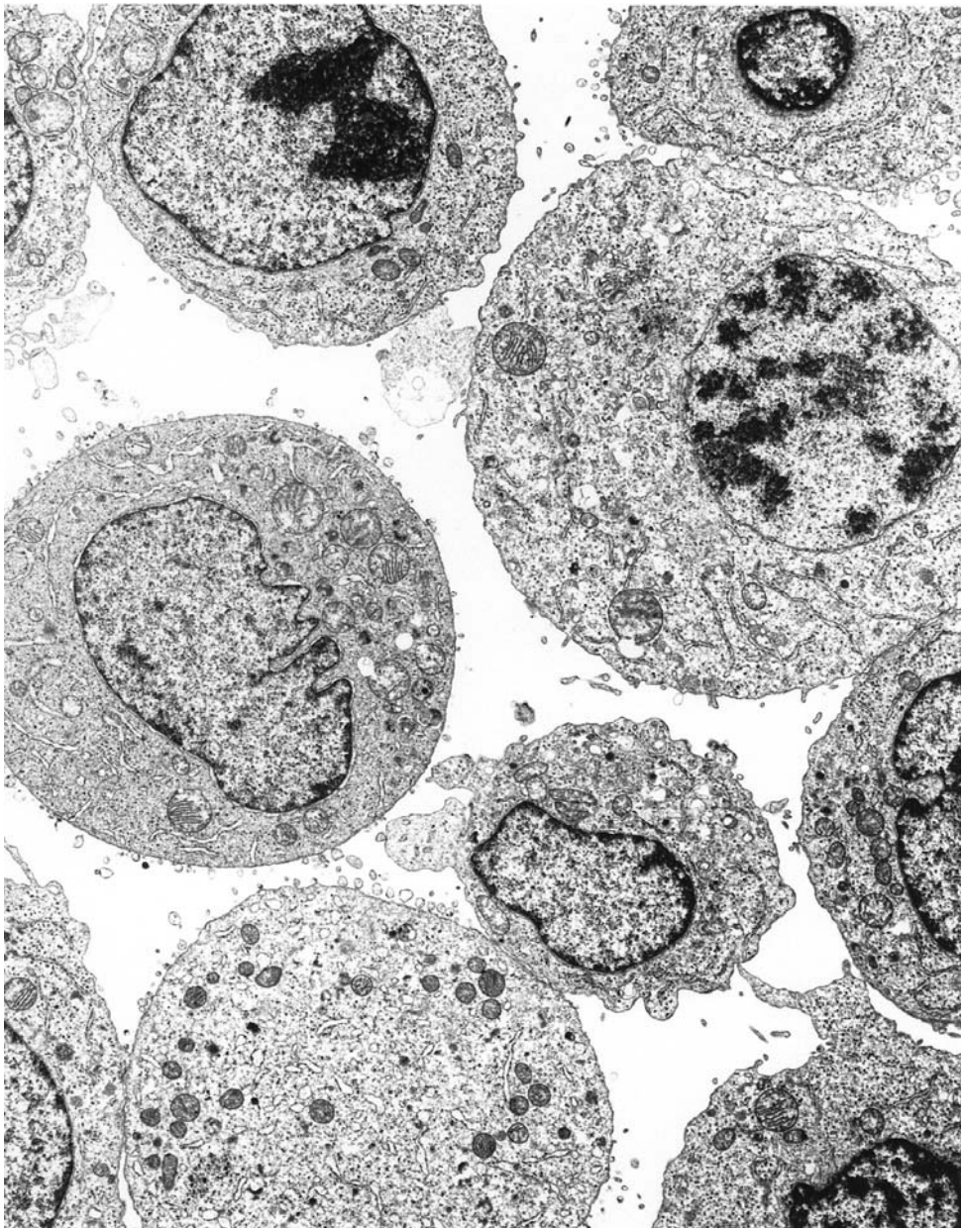

Figure 1. *Electron microscopy of U937 Cells undergoing replication 24 hr after adding fresh medium. Mitochondria are distributed throughout the cytoplasm, without evident juxta-nuclear concentration.(x 7300).*

storage and extra-cellular capacitative storage-related events, the latter dependent upon intra-cellular Ca^{2+}-depletion, would either be attenuated or circumvented altogether (*e.g.*, 27-33). Finally, in view of the absence in Bcl-2-negative Panc-1 and PC-3 cells of an acute nuclear Ca^{2+}-response to MK 886, despite comparable changes in mitochondrial membrane potential and induction of ROS (34), whether Bcl-2 could be implicated in the MK 886-induced rise in U937 nuclear Ca^{2+} was an additional point of interest (28, 29, 35-37).

Materials and Methods

Cell culture. U937 cells were cultured either in 25- or 75- cm^2 flasks at 37˚C with 5% CO_2 for the times indicated. The RPMI 1640 medium contained 10% FBS, 2 mM glutamine, 50 U/ml penicillin G, 50 μg/ml streptomycin and 25 mM HEPES. Cell viability was determined with trypan blue and a hemocytometer. MK 886 (3-(t-(4-chlorobenzyl-3-butyl) thioll-5-isopropylindiol-2-yl)-2,3-dimethyl propionic acid was stored at -70˚C as a 40 mM stock solution in dimethyl sulfoxide. Controls contained an identical

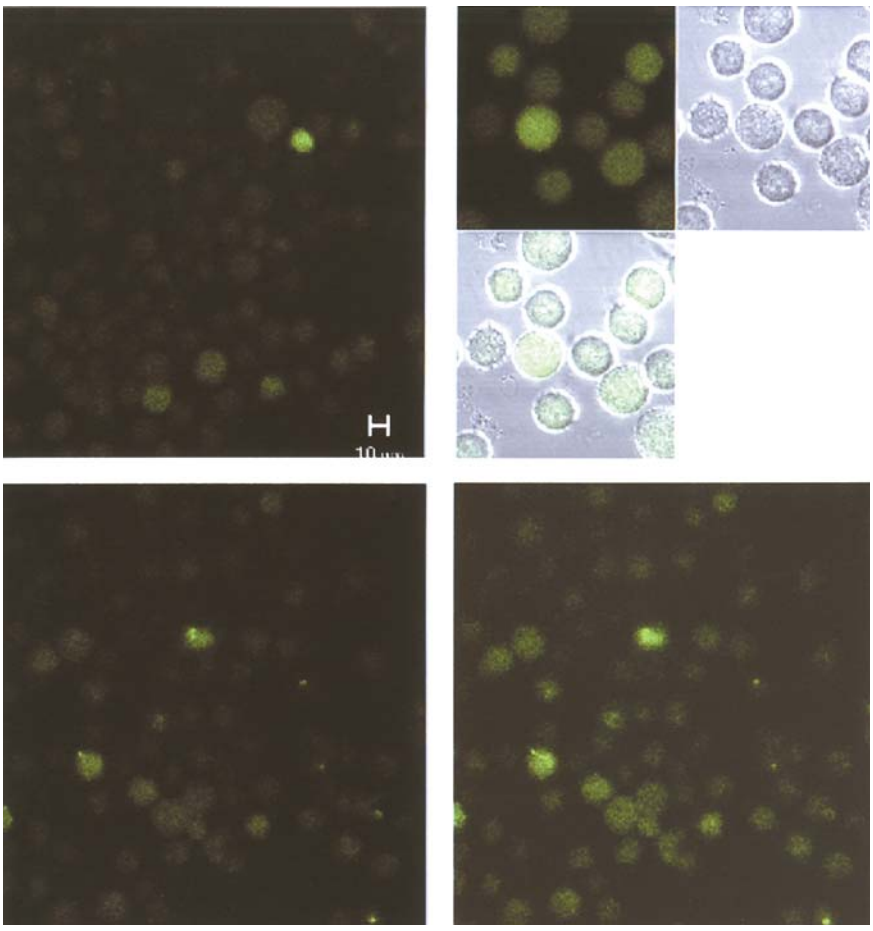

Figure 2. *Imaging of U937 Cells in Ca^{2+}-free medium, exposed to 40 μM MK 886 and examined with a Zeiss Confocal Microscope. Within 30 seconds of MK 886, a uniform "nuclear" fura-2-dependent fluorescence without peri-nuclear or cytosolic enhancement appeared, overlying the affected nuclei. Increases were not synchronous and most nuclei retained their initial fluorescence. "0"- to 3-minute images are presented (x 250). Insert, phase contrast overlays (x 400).*

concentration of the DMSO vehicle, 0.1% maximum, previously shown to have no effect on cell numbers.

Electron microscopy was performed according to conventional procedures.

Assay conditions for confocal microscopic Ca^{2+}, for ROS signaling studies and for radiometric Ca^{2+} studies with fura-2. Cells, washed in Ca^{2+} and Mg^{2+}-free Hanks buffer and adjusted in the same medium to at least 1 million cells / ml were incubated in the same buffer at 37˚C for 30 minutes with 2 μM of fura-2-AM, rhodamine-2-AM or 5(6) chloromethyl-2',7'-dichloro-dihydrofluorescein acetate (DCFDA) in Ca^{2+}-free Hank's buffer, washed twice with the same buffer at 2˚C. In some experiments, U937 cells were loaded together with fura-2-AM and BAPTA-AM.

Confocal microscopy. For confocal microscopy of fura-2, 340 excitation and 510 nm emission were employed (38,41); for rhod 2, excitation of 485 and emission of 590 nm (39,40). With DCFDC –loaded cells, we used excitations from an argon/krypton mixed gas laser with 488 excitation and 525 nm emission (42). Cells were loaded with dye, as described in Materials and Methods, placed on a planchette coated with Cell Tak and analyzed with an LSM 510 Zeiss Axiovert 100 M confocal microscope with the help of Dr. Chen, Director of the Confocal Facility of the University of Illinois at Chicago, U.S.A. A variety of controls including DMSO or cells alone, or in combination without drug, or simply exposure to incident radiation over the time course of an experiment were included.

For radiometric detection of fura-2, excitation at 340/380 nm and emission at 510 nm were used (38).The concentrations of enzymes and chemicals added before and after challenging fura-2-loaded cells with MK 886 are presented in Table I. The concentrations chosen were based on values available from the literature and were intended to try and restrict cellular response to the intended target and avoid more generalized effects.

Chemicals and tissue culture reagents were purchased from Sigma Biochemicals , St. Louis, MO, Calbiochem, San Diego, CA, Gibco-BRL, Bethesda, MD, Molecular Probes, Eugene, OR, Tocris, Ellisville, MO and BioMol, Plymouth Meeting, PA, U.S.A.

Results

Electron microscopy. To establish the location and qualitatively estimate the number of mitochondria in representative U937 cells late in their cell cycle, electron microscopy was employed.

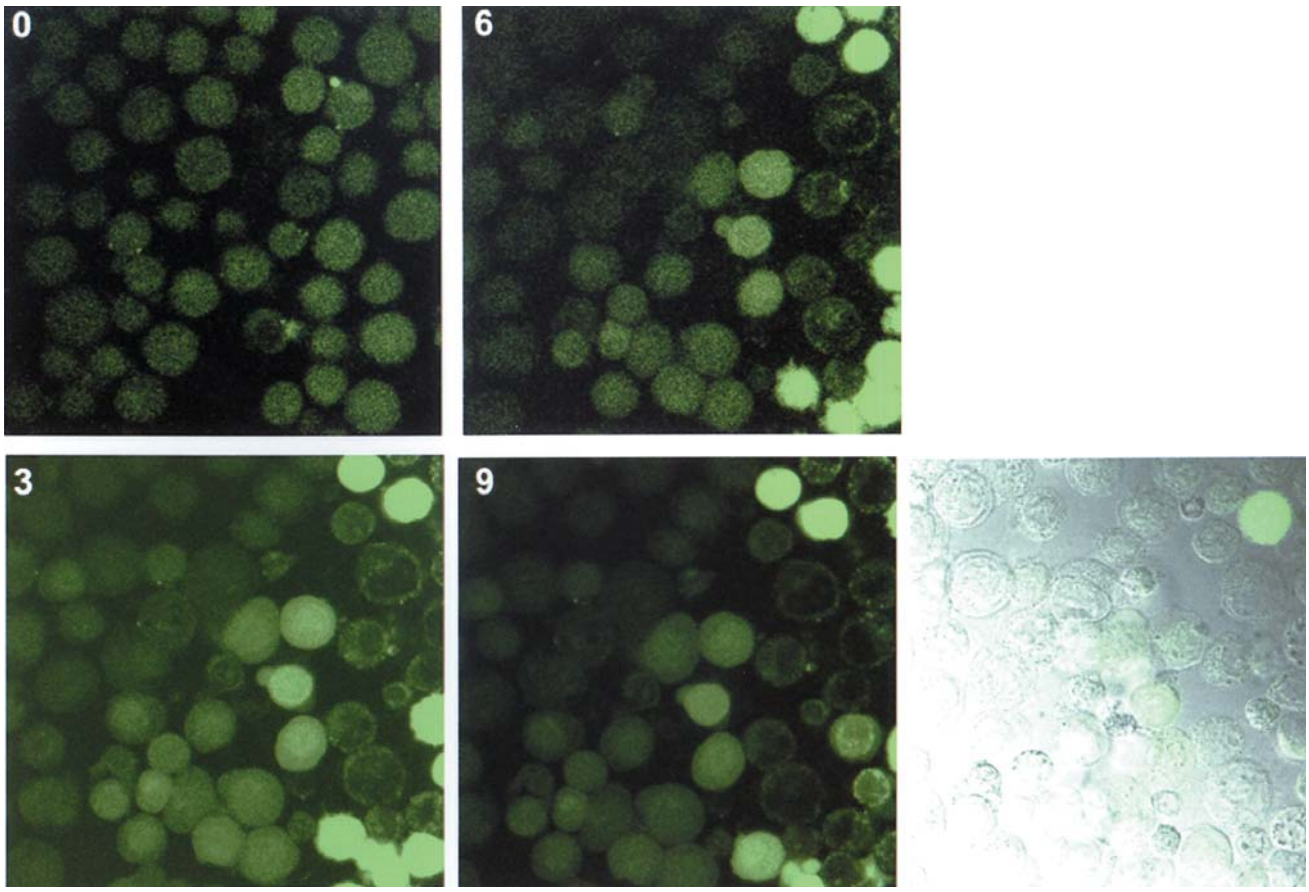

Figure 3. *Time course and intracellular location of Ca^{2+} appearance and turnover under the conditions of Fig. 2. After 3 to 5 or more minutes, occasional nuclei lost fluorescence, which concentrated in small rod to round or ovoid concentrations that migrated toward the plasma membranes. Intervals of 3, 6 and 9 minutes.*

In Figure 1, numerous mitochondria are evident, without any preferential concentration in the vicinity of nuclei in cells, many of which were completing cell division.

We then used confocal microscopy to examine the acute response to MK 886, defined as occurring within 10 or more seconds and measured for 3 to 5 minutes, of fura-2, rhod-2 or 2',7'-dichloro-dihydrofluorescein (DCFDA)-loaded U937 cells in Ca^{2+}-free medium. Subsequently, the ability of various agents of interest to alter the MK 886-induced Ca^{2+} -response was examined by radiometric spectrometry of fura-2-loaded cells (38).

Confocal microscopy with fura-2: kinetics of increased Ca^{2+} and its nuclear localization examined by the two-dimensional "Z"-stacking technique. Within 10 to 20 seconds of adding MK 886 to fura-2-loaded, Ca^{2+}-depleted U937 cells in Hank's Ca^{2+}-free buffer and attached to the planchette with Cell-Tak , an increased, rather uniform distribution of fluorescence rapidly appeared over the center of affected cells, encompassing individual nuclei (Figures 2, 3). No peri-nuclear halo or increased peri-nuclear or decreased cytosol fluorescence, were ibserved either before or after the increase of Ca^{2+}. A limited increase in cytosol fluorescence was also present in some cells exhibiting increased nuclear fluorescence. Increases in nuclear fluorescence were not synchronous and most nuclei retained their fluorescence. In some cells with relatively unstained nuclei, faint fluorescence of cytoplasmic structures compatible with mitochondria and the ER was present; why nuclei in these cells were unaffected was not clear. During the subsequent 3 to 10 minutes, fluorescence occasionally associated with nuclei became concentrated in smaller, rod-like bodies (Figure 3). Some of this fluorescence may have contributed to the particulate fluorescence that in a few cells subsequently migrated through the cytosol and to the plasma membrane. Often these changes occurred in cells

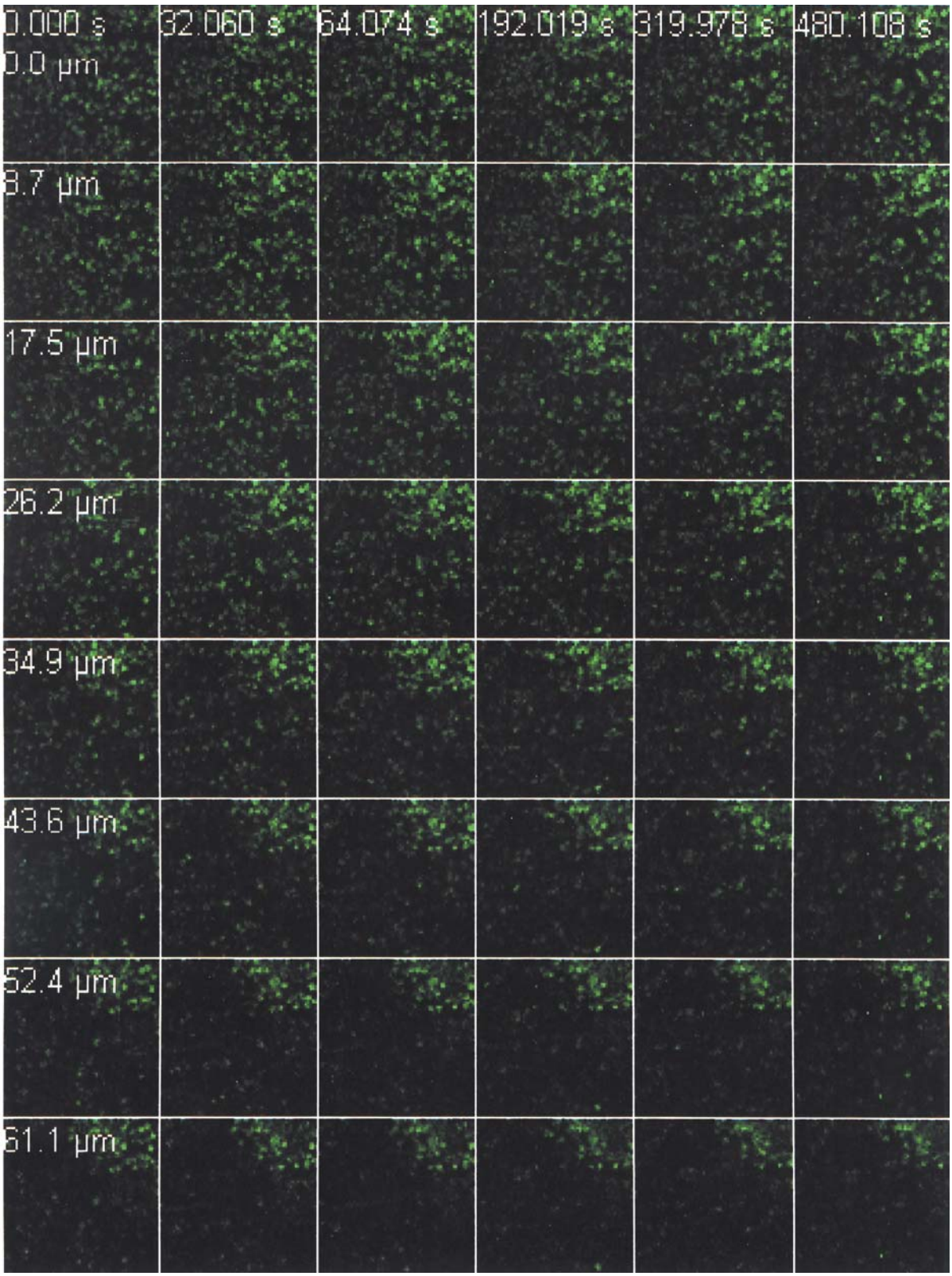

Figure 4. *Z-stacking procedure in which fura-2-labelled cells were analyzed over 480 seconds (x-axis) while images at different "cuts" (y-axis) through the cells from "0" to 61.1 µm we recorded. Note the relative constancy in location of increased fluorescence in individual cells, which can wax and wane as "cuts" are made through them. An initial total of 120 images were recorded, of which 64 are presented (x 250).*

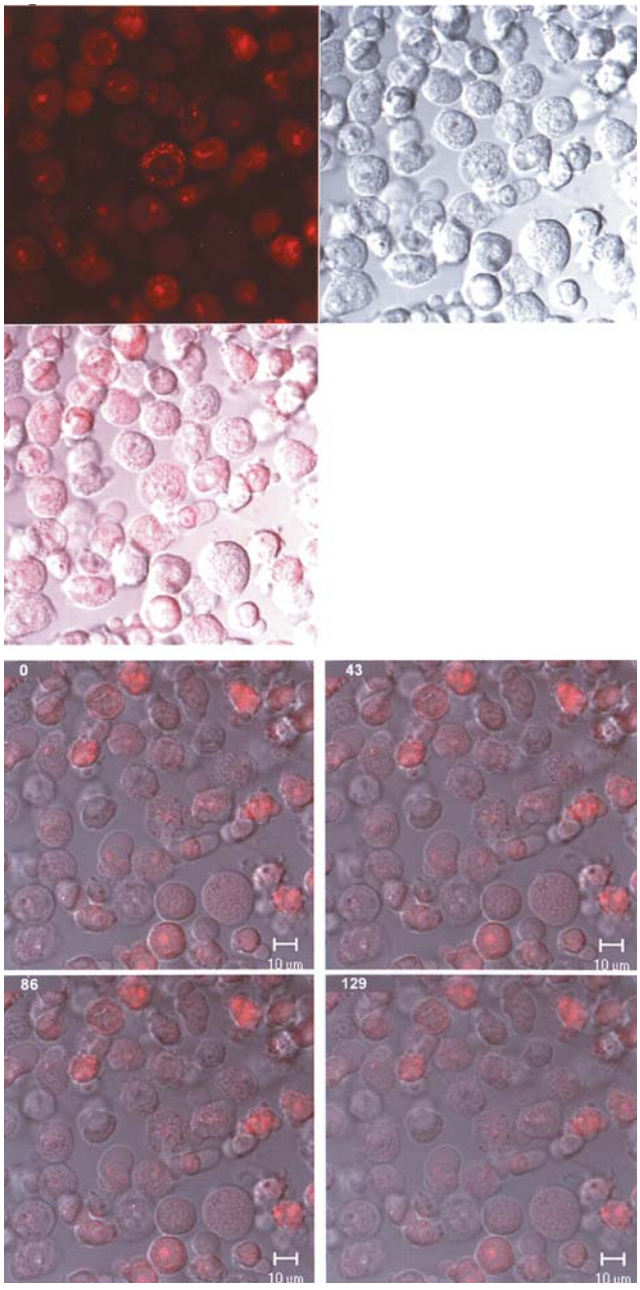

Figure 5. *Rhodamine-2 fluorescence of U937 cells in Ca^{2+}-free medium after 40 µM MK 886. Upper panel: Phase contrast demonstrating cytoplasmic and nucleolar location of fluorescence and its absence in the nucleoplasm (x 400). Lower panel: time course from 0, 43, 86 and 129 seconds following 40 µM MK 886 (x 400). Rhod-2 fluorescence is located primarily in the mitochondria, the extra-mitochondrial cytoplasm including the endoplasmic reticulum and in nucleoli excluding the nucleoplasm. In three separate experiments,this distribution did not visibly alter after addition of MK 886. Following MK 886, the fluorescence kinetics of nuclei (fura-2, Figs 2 and 3) and extra-nuclear regions differ.*

with plasma membrane blebbing and we considered these latter events a consequence of incipient cell death.

To further confirm the kinetics and nuclear location of the majority of the Ca^{2+} signal, fura-2-loaded cells challenged with MK 886 were examined over 8 minutes with successive confocal cross-sectioning from lower to upper surfaces of the cells (Figure 4; Z-stacking technique). During sampling, increased fluorescence appeared across the x-axis in a number of cells. Along the y axis, fluorescence increased through a central maximum, as sections were recorded from the bottom (0.0 µm), through the middle and finally reaching the upper surfaces (61.1 µm) of cells. Increases occurred without change in the developing central location of the major fluorescence, which could recede as the upper boundaries of analyzed cells were reached. Nuclear fluorescence was not observed to increase at the expense of cytoplasmic fluorescence. These results are consistent with the major increases in fluorescence occurring within their initial sites of origin, the cell nuclei, as defined earlier.

Confocal studies with Rhod-2-AM. Although fura-2 with a negative charge at neutral pH is less likely to localize in mitochondria, due to their mutual charge-relationships, Ca^{2+} responsible for the "nuclear" fluorescence might be due to a very rapid and difficult to observe release from that site or from the ER with diffusion to nuclei, giving the impression of a primary nuclear origin. Since rhodamine-2, a more lipophilic probe for Ca^{2+} with a positive charge around neutral pH, concentrates in mitochondria (39), we incubated rhod 2-loaded U937 cells with MK 886, as described for fura-2-AM (Figure 5).

Initially, a number of control cells exhibited discrete concentrations of fluorescing dye in rod-like structures consistent with the dimensions of mitochondria. Other cells had a more uniform distribution of fluorescence spread through extra-nuclear regions of the cell, including presumptive regions of the ER. With the exception of discrete nucleolar staining, nuclei were not fluorescent. After addition of 40 µM MK 886, fluorescence was measured at 20-second intervals for 5 minutes. Generally, in cells exhibiting more diffuse cytoplasmic fluorescence, little change occurred during this time and the nucleoplasm, apart from fluorescing nucleoli, which did not alter during the experiment, continued to be represented by a non-fluorescent nucleoplasmic "halo", separate from regions of cells that fluoresced. By 300 seconds, in a few cells, small foci of fluorescence migrated toward or even reached the plasma membranes. Some loss of cytoplasmic, including putative mitochondrial fluorescence occurred, in others cytosol fluorescence increased, or even became apparent in an occasional cell where none had been evident. We interpreted at least some of these later events as representing cells undergoing unfavorable events due to the

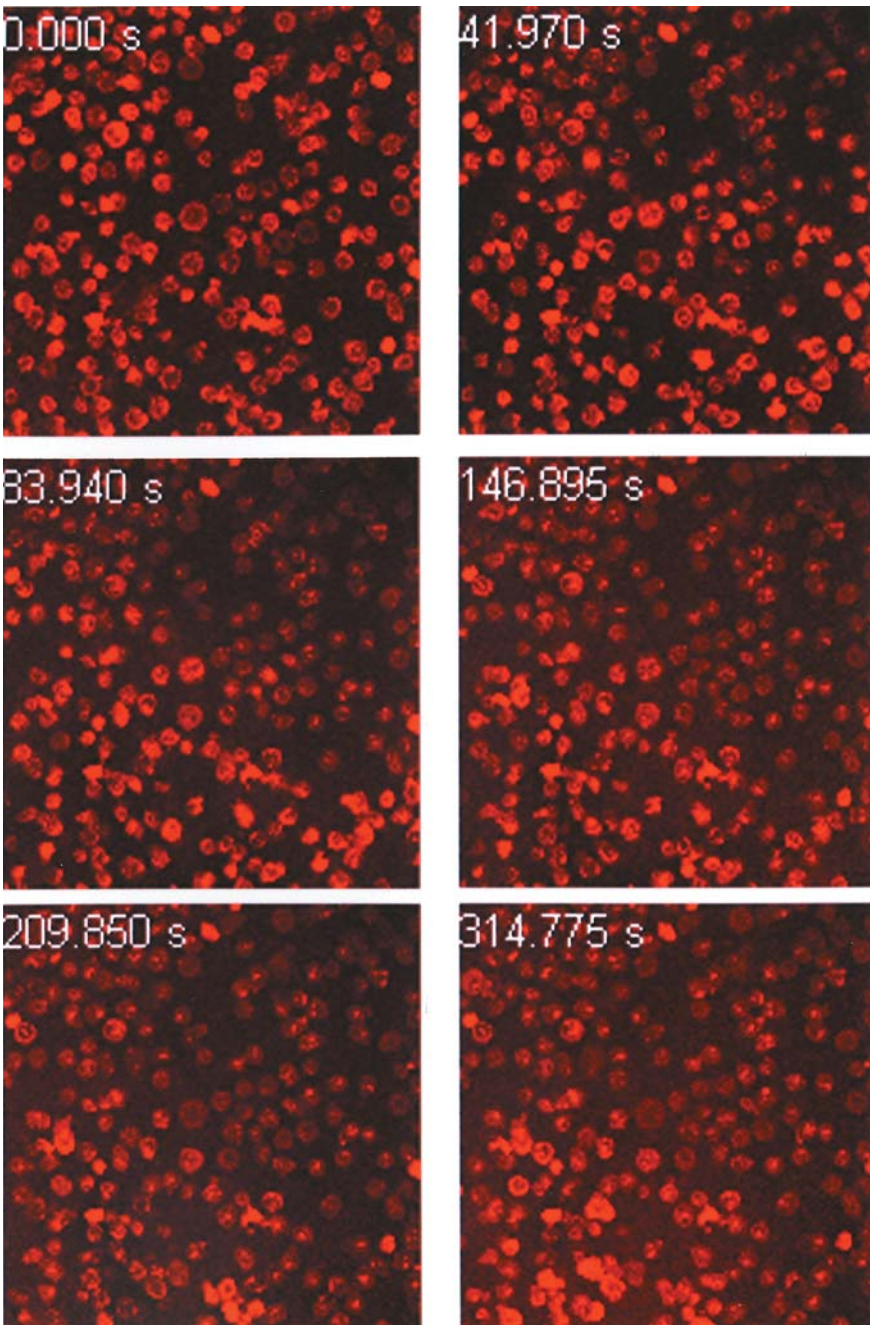

Figure 6. *Two,7-dichloro-dihydrofluorescein (DCDHF) fluorescence of U937 cells in Ca^{2+}-free medium after 40 μM MK 886. Careful observation over 366 seconds revealed dynamic changes in individual cells with the appearance and disappearance of fluorescence in a highly individualistic manner. Intensely fluorescent cells, especially those with centrally located fluorescence, may represent nuclear fluorescence, but in other cells, in which central nuclear fluorescence was minimal, cytosol fluorescence could appear and subsequently disappear. Generally, the majority of fluorescence appeared to be extra-nuclear. Of the 18 original images, 6 are shown (x 250).*

non-physiologic conditions toward the end of the experiment; cells maintained at 37˚C in Ca^{2+}-free medium and ambient (0.03%) CO_2.

With non-laser excitation of cells left on the microscope stage for prolonged periods of time, fluorescence could uniformly diminish in all compartments due to cell death with membrane blebbing, leakage of dye and possibly some photo-bleaching (43,44).

Detection with 2,7-dichloro-dihydrofluorescin of intracellular ROS and their rapid increase after MK 886. We employed the fluorescein dye, DCDHF, to detect sites of formation of reactive oxygen species such as hydrogen peroxide and a precursor, superoxide (42), both before and after exposure to MK 886. In control cells loaded with the dye, most cells fluoresced to some extent. These included cells with small, punctate regions consistent with mitochondria, in others as

more diffuse regions compatible with the ER and, finally, a few cells with intense fluorescence that encompassed most or all of the structure. After addition of 40 μM Mk 886, three types of change were evident (Figure 6). Within 30 seconds and subsequently for the 5 minutes of observation, fluorescence increased in some initially-labelled cells. These included cells that continued to exhibit "punctate" collections of fluorescence, cells with evident non-mitochondrial cytoplasmic fluorescence, up to and including cells in which an apparent "nuclear" fluorescence occupied much or even most of the center of the affected cells. Yet in many affected cells, nucleoplasmic fluorescence was not prominent. Additional cells, initially without much fluorescence, developed it up to several minutes after addition of the drug. Other cells lost fluorescence, in some associated with plasma membrane blebbing. Thus, changes in fluorescence as a measure of ROS formation varied markedly among the population of cells, exhibiting much more variability than those loaded with fura-2 or rhod-2.

Fluorescence spectrometry. In these studies, cells loaded with fura-2 were examined with the radiometric technique (38) before or after addition of MK 886 and any changes in Ca^{2+} monitored (Table I). Depending upon the agent employed, concentrations from 25 nM to 100 μM were used. Figure 7 is representative of the procedure employed, as described in Materials and Methods, in which N-acetyl- L-cysteine is shown to inhibit induction of a Ca^{2+}-response, while not significantly reducing the fluorescence once achieved.

Agents that did not acutely alter the rapid MK 886-induced Ca^{2+} increase in non-permeabilized U937-fura-2-labelled cells were examined in Ca^{2+}-free medium with a LS-40 luminescence spectrometer: Agents of interest, added for 50 seconds before addition of 40 μM MK 886, that did not alter the expected Ca^{2+} -response, are listed in Table I. These included H_2O_2, (oxidative stress), NTBN (free radical spin trap), 2-methylantimycin A3 (inhibits Bcl-2 function), SC41661A (redox inhibitor of 5-lipoxygenase), thapsigargin (ER ATPase) and ionomycin (Ca^{2+} ionophore), both able to increase cytosol Ca^{2+}, and nifedipine (L Ca^{2+} channel), sodium arsenate (uncoupler of oxidative phosphorylation), sodium cyanide (inhibits terminal respiration), MSH and DTT (antioxidants) and modulators of cAMP including caffeine, theophyllin and indomethacin.

The inability to reduce the MK 886-induced rise in Ca^{2+} with 10-50 nM wortmannin was unexpected. We also incubated cells with wortmannin at 37˚C for 1-2 hours without clear-cut inhibition. If the concentration was increased 100 or more fold, inhibition could occur, but cytotoxicity could not be excluded as the medium became intensely acidic.

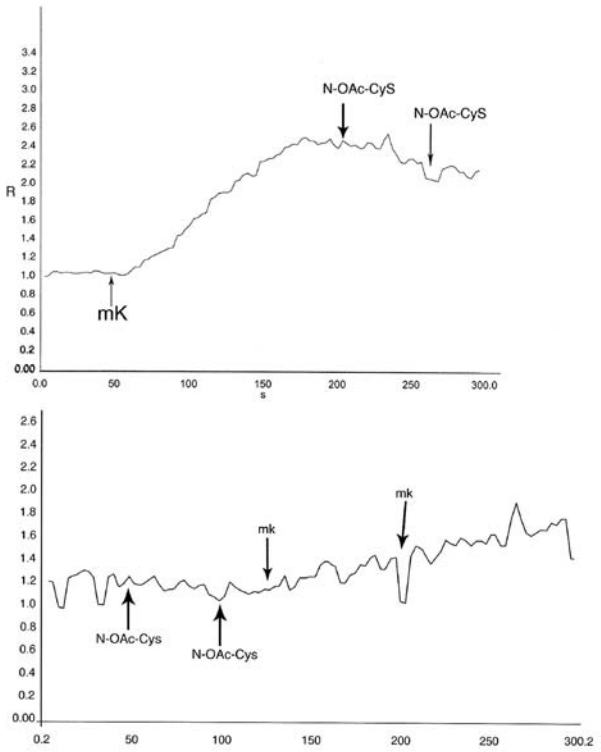

Figure 7. *A representative fluorescence spectrometry experiment in which suppression of the MK 886-induced Ca^{2+} signal by N-acetyl-cysteine before and lack of significant reduction after addition of 40 μM MK 886 is depicted. Individual spectrometry experiments listed in Table I were performed in a similar manner, generally repeated 3 or more times.*

Antioxidant agents unable to enter cells, including SOD, catalase and peroxidase, did not inhibit the Ca^{2+} response (45).

Agents acutely inhibiting the increase: Antimycin A (inhibitor of mitochondrial oxidative phosphorylation which can increase cytosol Ca^{2+}), atractyloside (inhibits oxidative phosphorylation and an agonist for initiating the mitochondrial membrane pore transition, MMP), loperamide (L/N-type Ca^{2+} channel), cyclosporine A (inhibits opening of mitochondrial membrane pores and Ca^{2+} release) and N-acetyl -L-cysteine, an antioxidant, all prevented or reduced the extent of the MK 886-induced rise in Ca^{2+}.

Response of U937 cells to BAPTA. To examine whether the intracellular Ca^{2+} chelator, BAPTA, inhibited the response of fura-2-loaded cells (46, 47), we preloaded cells with fura-2-AM and 25 or 100 μM BAPTA-AM (37˚C, 30 minutes) as described and subsequently added MK 886. In these experiments, no MK-886-induced increase in Ca^{2+} occurred (not shown). The basal concentrations of BAPTA-treated cells were less than that of the control cells and CCCP (carboxy cyanide p[trifluoromethoxy]phenyl

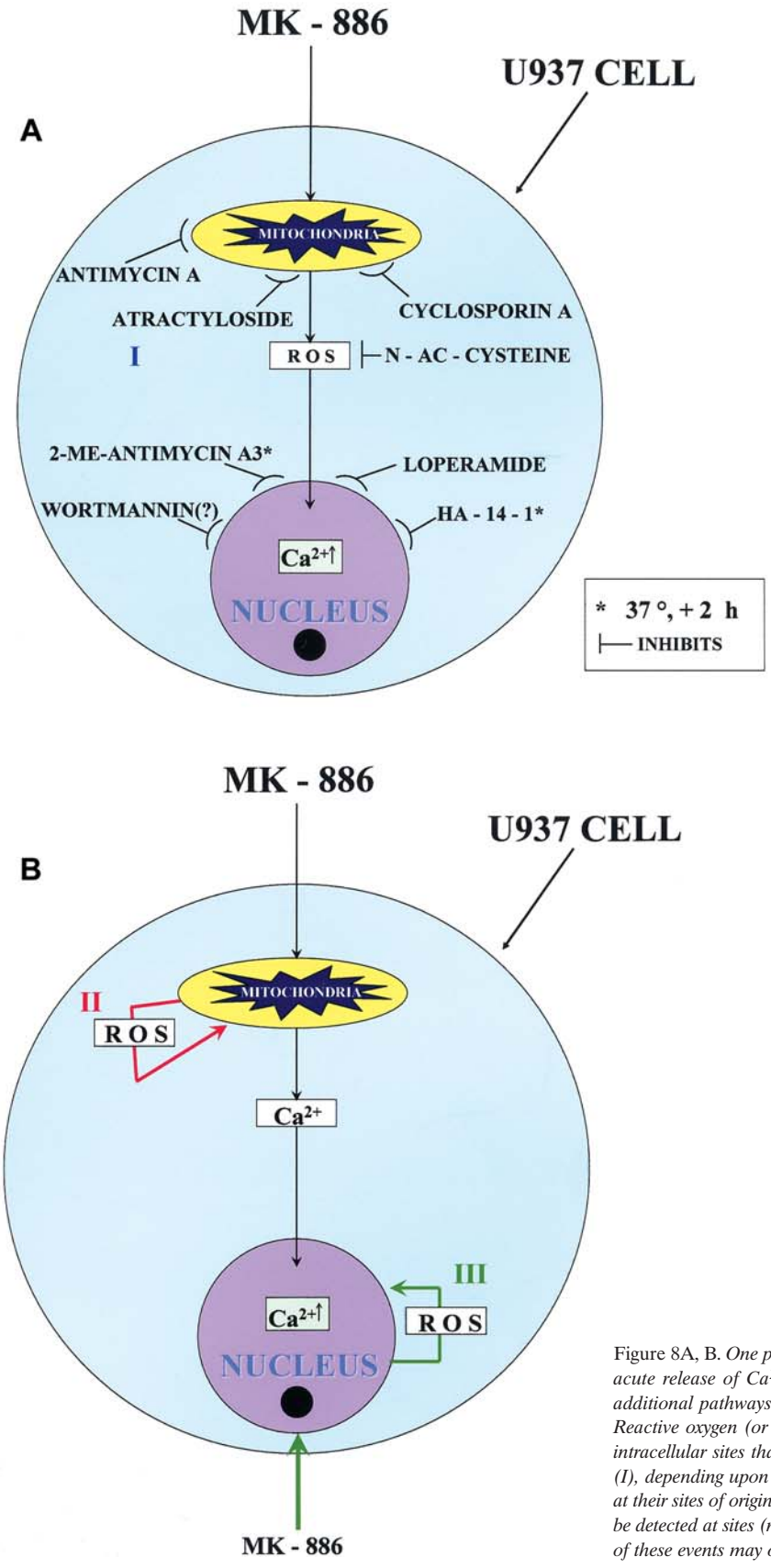

Figure 8A, B. *One proposed major pathway (I) thought to contribute to the acute release of Ca^{2+} from U937 nuclear sites by MK 886 (8A) and 2 additional pathways (8B; II, III) that may also participate are depicted. Reactive oxygen (or nitrogen) species generated in mitochondria or other intracellular sites that act either locally (II, possibly III) or more distantly (I), depending upon their half lives and other circumstances, release Ca^{2+} at their sites of origin (II,III) or more distantly (I), which can diffuse to and be detected at sites (nuclear, in particular) containing resident fura-2. Some of these events may occur asynchronously in the same or in different cells.*

hydrazone) at 10 μM evoked a robust Ca^{2+} signal in control cells, augmented by additional MK 886; in BAPTA-treated cells, both events were greatly reduced (not shown). BAPTA-AM added to established Ca^{2+} increases did not quench the signal.

A role for Bcl-2 in this "nuclear" Ca^{2+} signaling? A potential relationship between Bcl-2 and the immediate Ca^{2+} signaling in U937 cells was considered. Several agents, HA 14-1 (48) and 2-methoxy antimycin A_3 (49), which impair the function of Bc-2, were examined acutely as described and after culture at 37˚C. Two hours of culture with HA 14-1 inhibited the response to MK 886, but this was not found during an acute exposure. Prior culture for 2 hours with 3-0-methyl antimycin A3 delayed a rise in Ca^{2+} and partially attenuated the final response to MK 886. Acute exposure did not reduce or abolish the response.

The conclusions reached with some of these agents would probably be different had higher concentrations and longer exposure under more physiological conditions been employed. Almost all the agents examined exert multiple concentration -and time-dependent effects on cells, some of which are lineage-dependent.

Finally, as mentioned, MK 886 rapidly induces oxidative stress and reduces mitochondrial membrane potential in U937 cells. These events also occurred in Bcl-2-negative Panc-1 and PC-3 prostate cells, in which MK 886 did not acutely generate a Ca^{2+} signal (34).

Discussion

With the methodology employed and under the intentionally restrictive conditions of these experiments, we believe the following conclusions are warranted (Figure 8).

1. Reactive oxygen species following exposure to MK 886 are mechanistically central to the increase in nuclear Ca^{2+}, based on its inhibition by N-acetyl-L-cysteine and the results of imaging with 2',7'-dichloro-dihydrofluorescin, demonstrating their increased formation in many cells.

2. Mitochondria are implicated in the acute MK-886-induced rise in nuclear Ca^{2+}, as judged from its inhibition by antimycin A, with potential effects including inducing a chemical hypoxia, inhibition of oxidative phosphorylation at complex III, increased formation of ROS, inhibition of succinic oxidase, NADH oxidase and the mitochondrial pore permeability transition (MPPT) with reduced Ca^{2+} uptake and increase in its cytosolic concentration; by atractyloside, which inhibits the ADP/ATP translocase, mitochondrial adenine nucleotide transport, and as a mitochondrial membrane pore agonist, augmenting the release of cytochrome C and Ca^{2+}; and by cyclosporin A, which is reported to reduce respiration, prevents the "opening" of mitochondrial membrane pores , inhibits the 2B phosphatase, calcineurin, blocks Ca^{2+}-related ionomycin-induced apoptosis in BLB cells (50) and inhibits nitric oxide synthesis (51). Mitochondria serve as an important storage site for excess cytosol Ca^{2+}, released under circumstances including oxidative stress (52, 53), antimycin (54) or atractyloside (55). In addition, mitochondria serve as a major source of ROS and RNS (56).

3. MK 886 did not induce an evident change in cytosol fluorescence of rhod-2-loaded cells examined with confocal microscopy. The absence of fluorescence in the nucleoplasm of rhod-2-labelled cells presumably is due to a lack of retention of the probe at that site. The lack of a visually evident decline in non-nuclear fluorescence in rhod-2-labelled cells following addition of MK 886 supports the view that, under these conditions, most "nuclear" Ca^{2+} originates *in situ*, which can include the perinuclear membranes, encompassed lumen and nucleoplasm. The lack of altered nucleolar fluorescence in rhod-2-labelled cells after MK886 had been added indicates a differential regulation of Ca^{2+} at that site and the nucleoplasm.

4. BAPTA at 25 or 100 μM pre-loaded with fura-2 into cells, subsequently washed, prevented the rise in Ca^{2+}, as determined by radiometric detection. The previous result with rhod-2 suggests that no major diffusion of Ca^{2+} from extra-nuclear to nuclear sites occurred. The potential release of Ca^{2+} still resident at extra-nuclear sites may be less evident in cells washed and incubated in Ca^{2+}-free medium. BAPTA reduced the basal Ca^{2+} of treated cells (not shown) and may have partially depleted a relevant Ca^{2+} store due to its higher Kd for that ion. BAPTA can disrupt the mitochondrial membrane potential (57), release Ca^{2+} from mitochondria, reduce voltage-gated K^+ currents (58) and translocate and inhibit PKC (59). BAPTA might chelate Ca^{2+} released by MK 886-related ROS from peri- or intra-nuclear sites and so prevent its detection.

5. Murine liver cell nuclei exhibit a form of respiration with oxidative phosphorylation and generate ROS (60,61). Whether comparable events occur in U937 cell nuclei which thus become susceptible to inhibitors of mitochondrial function, does not seem to have been studied (8B, III).

6. In view of the inhibition of increased Ca^{2+} by loperamide, an L/N Ca^{2+} channel blocking agent, and assuming the absence of confounding effects, participation of an intra-cellular "channel" may be implicated (62).

7. Based on incubation at 37˚C with HA-14-1, a direct inhibitor of Bcl-2 (48) and with 2-methyl-antimycin A3, an agent that is not considered to inhibit oxidative phosphorylation but binds with and inhibits Bcl-2 (49), Bcl-2 may participate in the rise of nuclear Ca^{2+}. Bcl-2 and especially other members of this family of proteins, such as BAX, can participate in the formation of ion channels (63).

In earlier studies, it was demonstrated that MK 886 induces oxidative stress in FL5.12 IL-3-dependent murine prolymphoid cells (64), U937 monoblastoid, PC-3 prostate

and Panc-1 pancreatic cancer cells (34). High (10 μM or more) concentrations of MK 886 inhibit respiration, depolarize the mitochondrial membrane and cause an ionophoretic effect with increased uptake of mono and divalent cations (65). MK 886 may itself serve as an ionophore, whether directly or by disruption of lipophilic membranes is not established. The interplay between reductive (anoxic) and oxidative stress, inhibition of ATP synthesis and inhibition and uncoupling of respiration from ATP synthesis as they are affected by inhibitors of mitochondrial function, when identified, should render the individual effects of nuclear Ca^{2+} understandable. Inhibition of oxidative phosphorylation can be associated with formation of excess ROS and release of Ca^{2+} from mitochondria (66, 67). Uncoupled respiration with energetically "futile" cycling of electrons may be associated with formation by MK 886 of reactive oxidative species by mitochondria. Mitochondria generate ROS from multiple sites; 8 are cited in Table I of reference (68), affecting complex I through IV. Other sites for formation of ROS could be affected by MK 886 including NADPH oxidase, cytochrome p450 - dependent oxygenases or it might serve as a xenobiotic capable of inducing futile electron cycling associated with formation of ROS or RNS. The observed increases in ROS (RNS) occurred primarily at extra-nuclear regions, but in DCDHF-labelled cells dominated by the increase in non-nuclear fluorescence, nuclear participation was not excluded.

Acute exposure of U937 cells to antimycin A or atractyloside, which inhibit specific steps of oxidative phosphorylation but can have opposite effects on the MMPT or to cyclosporin A, which closes the "pore", each reduced or prevented the MK 886-induced acute rise in nuclear Ca^{2+} without themselves generating a Ca^{2+} signal. We speculate that the initial effects of antimycin A, atractyloside and cyclosporin A on mitochondrial function promoted the inhibition of ROS or RNS formation or release, rather than a major direct release of Ca^{2+} from mitochondria which we did not detect. Pre-treatment with antimycin A , atractyloside or BAPTA may deplete a mitochondrial Ca^{2+} store which is then unresponsive to subsequent MK 886 - induced oxidative stress. However, we should have detected an initial acute rise in Ca^{2+} preceding addition of MK886. The mitochondrial membrane permeability transition pore (MMPT), a major mitochondrial Ca^{2+} channel, is inhibited by Ca^{2+}, atractyloside, cyclosporin A, H^+ and other agents, a point against release of Ca^{2+} from that site (69). Closure by cyclosporin A of mitochondrial membrane "pores" should reduce the formation or release of ROS or RNS induced by MK 886. Ca^{2+} from the ER can be sequestered in mitochondria in association with increasing oxidative stress, leading to cell death (70,71). Whether MK 886 acutely depletes ATP pools was not measured; agents such as antimycin A can do so within several minutes of exposure. It has been suggested that the level of mitochondrial Ca^{2+} determines the fate of cells; high concentrations lead to necrosis, lower concentrations to apoptosis (72,73).

Differences in the initial responses to antimycin A and 2-methoxy-antimycin A3 distinguish events related to inhibition of oxidative phosphorylation accompanied by a limited rise in Ca^{2+} by the former from putative effects of the latter on Bcl-2 (Table I). A reduced MK 886-induced rise in nuclear Ca^{2+} after culture with 2-methoxy-antimycin A3 or HA14-1, which both interact with Bcl-2, suggests an association with Bcl-2 in these Bcl-2-positive U937 cells. With prolonged culture, these agents exert additional effects on cells resulting in programmed cell death. Inhibition of Bcl-2 should reduce its anti-oxidant activity (74), augmenting any ROS/RNS-dependent rise in Ca^{2+}. Since this was not observed, any putative Bcl-2 anti-oxidant activity seems mechanistically irrelevant. As Bcl-2 and some of its congeners can participate in the formation of ion channels, such channels may be present at or near nuclei and their membranes. Reduced nuclear Ca^{2+} by the L/N channel inhibitor, loperamide, directs future attention to this possibility.

The response to wortmannin was ambiguous and requires further study (75). When Dulbecco's Ca^{2+}-free phosphate buffer was used to prepare loaded cells, usually the response to MK 886 was much less compared with Hank's Ca^{2+}-free buffer. The phosphate concentration of Dulbecco's buffer is 2.36 g/l compared with 0.15 g/l in Hank's buffer, a 15.7-fold difference. This was probably responsible for greater depletion of Ca^{2+} from these cells. The use of CCCP to assess a release of Ca^{2+} from mitochondria was useful.

A number of potential complications can mislead the interpretation of confocal microscopy studies. These include the extent to which fluorescent probes are retained *in situ* or diffuse locally, auto-fluorescence, whether the ligand is released and appears at other sites, radiation-induced photo-bleaching and damage to cells, especially from laser excitation with the DCDHF probe, quenching due to excess probe or its metabolites or loss of a probe or ligand from cells (43,44). However, from the results with fura-2 and rhod-2 imaging, we believe most of the increased nuclear Ca^{2+} induced by MK 886 originated from calcium present *in situ*, including the peri-nuclear endoplasmic reticulum, its membranes, lumen and any extensions into the nucleoplasm (12, 22; Figure 8A, I),

The lack of a Ca^{2+} -response to MK 886 in Bcl-2-negative epithelial cancer cell-derived Panc-1 and PC-3 cells and its presence in Bcl-2-positive U937 and HL-60 cells is striking. In the Dunning rat prostate model, Bcl-2 reduced nuclear uptake of Ca^{2+} (6). Whether modulation of nuclear Ca^{2+} by Bcl-2 depends upon the lineage of the cells studied or is a more general property is not defined.

Overall the evidence leads us to favor the formation of ROS induced by MK 886 at the most likely site, the mitochondria, their diffusion to nuclei and release of significant Ca^{2+} at that site (Figure 8A, I). It can be argued that opening of the MMPT by MK 886, loss from mitochondria with diffusion of Ca^{2+} to nuclei may contribute at some point, but we have no definite evidence of this (Figure 8B, II). Finally, MK 886 might induce synthesis of ROS by nuclei with release of Ca^{2+} from that and contiguous structures (Figure 8B, III and ref 76).

Whether increase in nuclear Ca^{2+} due to MK 886 alters nuclear transcription, and the effect of directly reducing U937 Bcl-2 protein on nuclear Ca^{2+}, are considerations for future studies. However, further identifying the sites and mechanism by which MK 886 induces increased ROS or RNS, the mechanism of release of Ca^{2+} from putative nuclear sites, structures including enzymes with which it associates and any consequences for early transcription underlying inhibition of replication and programmed cell death remain to be defined.

Acknowledgements

We thank the Weinberg Foundation, the Seidel Family Trust and the Wadsworth Memorial Trust for their continued support. We also thank Dr. C. Chen , Director, The Flow Cytometry Laboratory of the University of Illinois Research Resources Committee for her aid in the studies with that instrument. We also thank Ms. Yunming Hu and Dr. Sergi Jadko for their expert technical assistance.

References

1 Scaffidi C, Kirchhoff S, Krammer PH and Peter ME: Apoptosis signaling in lymphocytes. Curr Opin Immunol *11*: 277-285, 1999.
2 Anderson KM, Seed T, Jajeh A, Dudeja P, Byun T, Meng J, Ou D, Bonomi P and Harris JE: An *in vivo* inhibitor of 5-lipoxygenase, MK 886, at micromolar concentration induces apoptosis in U937 and CML cells. Anticancer Res *16*: 2589-2600, 1996.
3 Alrefai W, Anderson KM, Bonomi P, Hu Y, Ou D and Harris JE: Acute changes in U937 nuclear Ca^{2+} induced to undergo programmed cell death by MK 886. Proc Am Assoc Can Res *44*: #5037, 1155, 2003.
4 Anderson KM, Alrefai W, Bonomi P, Seed T, Dudeja P, Hu Y and Harris JE: Caspase-dependent and independent panc-1 cell death due to actinomycin D and MK 886 are additive but increase clonogenic survival. Exp Biol Med *228*: 915-925, 2003.
5 Kleeff J, Kornmann M, Sawhney H and Korc M: Actinomycin D induces apoptosis and inhibits growth of pancreatic cancer cells. Int J Cancer *86*: 399-407, 2000.
6 Marin MC, Fernandez A, Bick RJ, Brisbay S, Buja LM, Snuggs M, McConkey DJ, von Eschenbach AC, Keating MJ and McDonnell TJ: Apoptosis suppression by bcl-2 is correlated with the regulation of nuclear and cytosolic Ca^{2+}. Oncogene *12*: 2259-2266, 1996.
7 Allbritton NL, Oancea E, Kuhn MA and Meyer T: Source of nuclear calcium signals. PNAS US *91*: 12458-12462, 1994.
8 Bzadminton MN, Campbell AK and Rembold CM: Differential regulation of nuclear and cytosol Ca^{2+} in HeLa cells. JBC *271*: 31210-31214, 1996.
9 Santella L and Carafoli E: Calcium signaling in the cell nucleus. FASEB J *11*: 1091-1109, 1997.
10 Petersen OH, Garasimenko OV, Gerasimenko JV, Mogami H and Tepikin AV: The calcium store in the nuclear envelope. Cell Calcium *23*: 87-90, 1998.
11 Lee MA, Dunn RG, Clapham DE, Stehno-Bittel J: Calcium regulation of nuclear pore permeability. Ibid, 91-101.
12 Hardingham GE, Cruzalegui FH, Chawlie S and Bading H: Mechanisms controlling gene expression by nuclear calcium signals. Ibid, 131-134.
13 Nicotera P and Orrenius S: The role of calcium in apoptosis. Ibid, 173-180.
14 Hardingham GE, Chawla S, Johnson CM and Bading H: Distinct functions of nuclear and cytoplasmic calcium in the control of gene expression. Nature *385*: 260-265,1997.
15 Fang M, Zhang H, Xue S, Li N and Wang L: Intracellular calcium distribution in apoptosis of HL-60 cells induced by harringtonine: intranuclear accumulation and regionalization. Cancer Lett *127*: 113-121, 1998.
16 Liu PPY, Kong SK, Kwok TT and Lee CY: The nuclei of He La cells contain tubular structures for Ca^{2+} signaling. Bio Bio Res Comm *247*: 88-93, 1998.
17 Rogue PJ and Malviya AN: Calcium signals in the cell nucleus; Strasbourg, France, Aug, 1998. EMBO J *18*: 5147-5152, 1999.
18 Van Den Brink GR, Bloemers SM, Van Den Blink B, Tertoolen LG, Van Deventer SJ and Peppelenbosch MP: Study of calcium signaling in non-excitable cells. Micro Res Tech *46*: 418-433, 1999.
19 Ermak G and Davies KJA: Calcium and oxidative stress: from cell signaling to cell death. Mol Immunol *38*: 713-721, 2001.
20 Dolmetsch RE, Pajvani U, Fife K, Spotts JM and Greenberg ME: Signaling to the nucleus by an L-type calcium channel-calmodulin complex through the MAP kinase pathway. Science *294*: 333-339, 2001.
21 Herr I and Debatin K-M: Cellular stress response and apoptosis in cancer therapy. Blood *98*: 2603-2614, 2001.
22 Feske S, Giltnane J, Dolmetsch R, Staudt LM and Rao A: Gene regulation mediated by calcium signals in T lymphocytes. Nat Immunol *2*: 316-324, 2001.
23 Shahin V, Danker T, Enss K, Ossig R and Oberleithner H: Evidence for Ca^{2+} and ATP-sensitive peripheral channels in nuclear pore complexes. FASEB J *15*: 1895-1901, 2001.
24 Hajnoczky G, Davies E and Madesh M: Calcium signaling and apoptosis. BBRC *304*: 445-454, 2003.
25 Echevarria W, Leite MF, Guerra MT, Zipfel WR and Nathanson MH: Regulation of calcium signals in the nucleus by a nucleoplasmic reticulum. Nat Cell Biol *5*: 440-446, 2003.
26 Leite MF, Thrower EC, Echefarria W, Koulen P, Hirata K, Bennett AM, Ehrlich BE and Nathanson MH: Nuclear and cytoplasmic calcium are regulated independently. PNAS US *100*: 22975-2980, 2003.
27 Stehno-Bittel L, Perez-Terzic C and Clapham DE: Diffusion across the nuclear envelope inhibited by depletion of nuclear Ca^{2+} stores. Science *270*: 1835-1838,1995.
28 Lam M, Dubyak G, Chen L, Nunez G, Miesfeld RL and Distelhorst CW: Evidence that Bcl-2 represses apoptosis by regulating endoplasmic reticulum-associated Ca^{2+} fluxes. PNAS US *91*: 6569-6673, 1994.

29 Zhang M, Zhang HQ and Xue SB: Effect of Bcl-2 and caspase 3 on calcium distribution in apoptotic HL-60 cells. Cell Res *10*: 213-220, 2000.

30 Babcock DF, Herrington J, Goodwin PC, Park YB and Hille B: Mitochondrial participation in the intracellular Ca^{2+} network. J Cell Biol *136*: 833-844, 1997.

31 Sartor VS and Duffy-Barbe L: Calcium store depletion induced by mitochondrial uncoupling in prostate cells. Gen Physiol Biophysics *19*: 265-278, 2000.

32 Schild L, Keilhoff G, Augustin W, Reiser G and Striggow F: Distinct Ca^{2+} thresholds determine cytochrome C release or permeability transition pore opening in brain mitochondria. FASEB J *15*: 565-567, 2001.

33 Bowser DN, Petrou S, Panchal RG, Smart ML and Williams DA: Release of mitochondrial Ca^{2+} *via* the permeability transition activates endoplasmic reticulum uptake. FASEB J *16*: 1105-1107, 2002.

34 Anderson KM, Alrefai WA, Dudeja PK, Jadko S, Bonomi P, Hu Y, Ou D and Harris JE: Increased cytosol Ca^{2+} and type 1 programmed cell death in Bcl-2-positive U937 but not in Bcl-2-negative PC3 and Panc-1 cells induced by the 5-lipoxygenase inhibitor MK 886. Prost Leuk Ess Fatty Acids *66*: 443-452, 2002.

35 Zhu L, Ling S, Yu X-D, Venkatesh LK, Subramanian T, Chinnadurai G and Kuo TH: Modulation of mitochondrial Ca^{2+} homeostasis by Bcl-2. JBC *274*: 33267-33273, 1999.

36 Williams SS, French JN Gilbert M, Rangaswami AA, Walleczek J and Knox SJ: Bcl-2 over-expression results in enhanced capacitative calcium entry and resistance to SKF-96395-induced apoptosis. Cancer Res *60*: 4358-4361, 2000.

37 Foyouzi-Youssefi R, Arnaudeau S, Borner C, Kelley WL, Tschopp J, Lew DP, Demaurex N and Krause K-H: Bcl-2 decreases the free Ca^{2+} concentration within the endoplasmic reticulum. PNAS US *97*: 5723-5728, 2000.

38 Grynkiewuicz G, Peonne M and Tsie RX: A new generation of Ca^{2+} indicators with greatly improved fluorescent properties. JBC *260*: 34430-34450, 1988.

39 Boitier E, Rea R and Duchen MR: Mitochopndria exert a negatigve feedback on the propagation of intracellular Ca^{2+} waves in rat cortical astrocytes. J Cell Biol *145*: 795-808, 1999.

40 Patel S, Robb-Gaspers LD and Thomas AP: Measuring single cell and subcellular Ca^{2+} signals. In: Calcium Signaling. JWE Putney, Ed, CRC Press, NY, pgs 343-363, 1999.

41 Roe MW, Lemasters JJ and Herman B: Assessment of fura-2 measurement of cytosolic free calcium. Cell Cal *11*: 63-73,1990.

42 Royall JA and Ischiropoulos H: Evaluation of 2',7'-dichlorofluorescin and dihydrorhodamine 123 as fluorescent probes for intracellular H_2O_2 in cellular endothelial cells. Arch Bio Bio *302*: 348-355, 1993.

43 Blatter LA and Wier WG: Intracellular diffusion, binding and compartmentalization of the fluorescent calcium indicators indo-1 and fura-2. Biophysical J *58*: 1491-1499, 1990.

44 Takahashi A, Camacho P, Lechleiter JD and Herman B: Measurement of intracellular calcium. Physio Rev *79*: 1089-1125, 1999.

45 Jou MJ, Jou SB, Chen HM, Lin CH and Peng TI: Critical role of mitochondrial reactive oxygen species formation in visible laser irradiation-induced apoptosis in rat brain astrocytes (RBA-1). J Biomed Sci *9*: 507-516, 2002.

46 Teufelhofer O, Weics R-M, Purzefall W, Schutte-Herman R, Micksche M, Berger W and Elbing L: Promyelocytic HL-60 cells express NADPH oxidase and are excellent targets in a rapid spectrophotometric microplate assay for extra-cellular superoxide. Tox Sci *781*: 376-383, 2003.

47 Robertson LE, Chubb S, Meyn RE, Story M, Ford R, Hittelman WN and Plunkett W: Induction of apoptotic cell death in chronic lymphocytic leukemia by 2-chloro-2-deoxyadenosine and 9-B-D-arabinoxyl-2-fluoroadenine. Blood *81*: 143-150, 1003.

48 Yoshida A, Ueda T, Takauji R, Liu Y-P, Fukushima T, Inuzuka M and Nakamura T: Role of calcium ion in induction of apoptosis by etoposide in human leukemia HL-60 cells. Biochem Biophys Res Commun *196*: 927-934, 1993.

49 Wang J-L, Liu D, Zhang Z-J, Shan S, Han X, Srinivasula SM, Croce CM, Alnemri ES and Huang Z: Structure-based discovery of an organic compound that binds Bcl-2 protein and induces apoptosis of tumor cells. PNAS US *97*: 7124-7129, 2000.

50 Tzung S-P, Kim KM, Basanez G, Giedt CD, Simon J, Zimmerbeerg J, Zhang KYJ and Hockenberry DM: Antamycin A mimics a cell death-inducing BCL-2 homology domain 3. Nat Cell Biol *3*: 185-181,2001.

51 Donjerkovic D, Zhang L and Scott DW: Regulation of p27 Kip1 accumulation in murine B-lymphona cells: role of c-myc and calcium. Cell Grow Diff *10*: 695-704,1999.

52 Firat DJ, Lynch RC and Leu RW: Cyclosporin A inhibits nitric oxide production by L- 929 cells in response to tumor necrosis factor and interferon-gamma. J Intfer Res *13*: 235-240, 1993.

53 Turrens JF: Mitochondrial formation of reactive oxygen species. J Physiol *552.2:* 335-344, 2003.

54 Byrne AM, Lemasters JJ and Nieminen AL: Contribution of increased mitochondria free Ca^{2+} to the mitochondrial permeabilitiy transition induced by tert butylhydroperoxide in rat hepatocytes. Hepatology *29*: 1523-1531, 1999.

55 Guidarelli A, Fiorani M and Cantoni O: Calcium-dependent mitochondrial formation of species promoting strand scission of genomic DNA in U937 cells exposed to tert-butylhydroperoxide: the role of arachidonic acid. Free Rad Res *33*: 477-487, 2000.

56 Stout AK, Raaaphael HM, Kanterewicz BI, Klann E and Reynolds IJ: Glutamate induced neurone death required mitochondrial calcium uptake. Nature Neuro *1*: 366-373, 1998.

57 Radi RR, Cassina A, Hodara R, Quijano C and Castro L: Peroxynitrite reactions and formation of mitochondria. Free Rad Biol Med *33*: 1451-1464, 2002.

58 Zhang M, Li Y and Xue S: BAPTA blocks DNA fragmentation and chromatin condensation downstream of caspase-3 and DFF activation in HY-induced apoptosis in HK-60 cells. Apoptosis *6*: 291-297, 2001.

59 Yuan XJ, Sugiyama T, Goldman WF, Rubin LJ and Blaustein MP: A mitochondrial uncoupler increases Kca currents but decreases KV currents in pulmonary artery myocytes. Am J Physiol *270*: C321-331, 1996.

60 Dieter P, Fitzke E and Duyster J: BAPTA induces a decrease in intracellular free calcium and a translocation and inactivation of protein kinase C in macrophages. Biol Chem Hoppe Seyler *374*: 171-174, 1993.

61 Yusa T, Crapo JD and Freeman BA: Hyperoxia enhances lung and liver nuclear superoxide generation. Biochim Biophys Acta *798*: 167-174, 1984.

62 Kukielka E and Cederbaum AI: NADPH- and NADHJ-dependent oxygen radical generation by rat liver nuclei in the presence of redox cycling agents and iron. Arch Biochem Biophys *283*: 326-333, 1990.
63 Church J, Fletcher EJ, Abdah-Hamid K and MacDonnald JF: Loperamide blocks high voltage-activated calcium channels and N-methyl-D-aspartate-evoked responses in rat and mouse cultured hippocampal pyramidal neurones. Mol Pharm *45*: 747-757, 1994.
64 Schendel SL, Xhe Z Montal MO, Matsuyano S and Montal M: Channel formation by antiapoptotic Bcl-2. Proc Nat Acad Sci US *94*: 5113-5118, 1997.
65 Datta K, Buswal SS and Kehrer JP: The 5-lipoxygenase activating protein (FLAP) induces apoptosis independently of FLAP. Bio J *34*: 371-375, 1999.inhibitor, MK 886
66 Gugliucci A Ranzato L, Scorrano L, Colonna R, Petronilli V, Cusan C, Prato M, Mancini M, Pagano F and Bernardi P: Mitochondria are direct targets of the lipoxygenase inhibitor MK 886. JBC *277*: 31789-31795, 2002.
67 Collins TJ, Lipp P, Beveridge MJ, Li W and Bootman MD: Inositol 1,4,5 trisphosphate-induced Ca^{2+} release is inhibited by mitochondrial depolarization. Biochem J *347*: 593-600, 2000.
68 Droge W: Free radicals in the physiologic control of cell function. Physiol Rev *82*: 47-95, 2002.
69 Turens JF: Mitochondrial formation of reactive oxygen species. J Physiol *552.2*: 335-344, 2003.
70 Jacobson J and Duchen MR: Mitochondrial oxidative stress and cell death in astrocytes - requirement for stored Ca^{2+} and sustained opening of the permeability transition pore. J Cell Sci *115*: 1175-1188, 2001.
71 Kowaltowski AJ, Castillo RF and Vercesi AE: Mitochondrial permeability transition and oxidative stress. FEBS Lett *495*: 12-15, 2001.
72 Ly JD, Grubb DR and Lawen A: The mitochondrial membrane potential (/\ym) in apoptosis; an update. Apoptosis *8*: 115-128, 1993.
73 Zhu LP, Yu XD, Brown RA and Kuo TH: Mitochondrial Ca^{2+} homeostasis in the regulation of apoptotic and necrotic cell deaths. Cell Cal *28*: 107-117, 2003.
74 Hockenberry DM, Oltivai ZN, Yin X-M, Millman CL and Korsmeyer SJ: Bcl-2 functions in an antioxidant pathway to prevent apoptosis. Cell *75*: 241-251, 1999.
75 Szalai G, Krishnamurthy R and Hajinoczky G: Apoptosis driven by IP 3-linded mitochondrial calcium signals. EMBO J *18*: 6349-6361, 1999.
76 Himpens B, DeSmedt H and Castels R: Kinetics of nucleoplasmic Ca^{2+} transients in DDT 1 MF-2 smooth muscle cells. Am J Physiol *263*: C978-985, 1992.

Received April 28, 2004
Accepted June 19, 2004